ACTIVE CONTOUR MODEL USING FRACTIONAL SINC WAVE FUNCTION FOR MEDICAL IMAGE SEGMENTATION

NORSHALIZA KAMARUDDIN

ABSTRACT

Intensity inhomogeneity occurs when pixels in medical images overlap due to anomalies in medical imaging devices. These anomalies lead to difficult medical image segmentation. This study proposes a new active contour model (ACM) with fractional sinc function to inexpensively segment medical images with intensity inhomogeneity. The method integrates a nonlinear fractional sinc function in its curve evolution and edge enhancement. The fractional sinc function contributes in giving a rapid contour movement where it improves the curve's bending capability. Furthermore, the fractional sinc function enables the contour evolution to move toward the object based on the preserved edges. This study uses the proposed method to segment medical images with intensity inhomogeneity using five various image modalities. With improved speed, the proposed method more accurately segments medical images compared with other baseline methods.

Keywords: level set method, nonlinear diffusion, active contour model, distance measurement, local or global properties

INTRODUCTION

The level of noise and level of intensity are the two main factors that lower the quality of medical images (Li, 2005, 2008; Patil & Deore, 2013; Xu, 2000). A problem called intensity inhomogeneity causes a non-uniform distribution of intensity in medical images that leads to difficulty in medical image segmentation (Hafiane et al., 2014; He et al., 2010; Kass et al., 1988). The most common segmentation technique called active contour model (ACM) uses a Gaussian filter with linear diffusion method isused to smooth the inhomogeneous image texture in medical images (Caselles et al., 1997; Kass et al., 1988; Li et al., 2010). However, the linear method also removes important information regarding image details, such as the small edges at object boundaries, which may lead to boundary leakages (Hafiane et al., 2014; Perona & Malik, 1990; Barenblatt, 2001; Barenblat & Vanquez, 2004). The basic idea of ACM is to progressively evolve a contour from its initial location in an image by following the trails of computed image pixel intensity or gradient in search of a complete object boundary (Kass et al., 1988; Xu et al., 2000; Caselles, 1997). Hence, the ACM fails to progress at the missing edge boundary. In contrast, the nonlinear diffusion method steers the diffusion at each image point, thereby preserving each edge and maintaining the structure of image details (Barenblatt, 2004; Sertan & Aydin, 2015).

The literature shows a number of studies that use the nonlinear diffusion function in image segmentation (Dan et al., 2012; Mahmoodi, 2003; Li et al., 2010; Wang, 2008) to smooth an image texture and maintain its edge structure. Studies in ACM that utilize this function started with the proposal of Perona-Malik. The Perona-Malik approach proposes the function's application in the anisotropic scale-space (Perona & Malik, 1990). Their work aims to reduce image noise without removing the image content (i.e. edges, lines, and other details) which is significant for image interpretation. The smoothing process in inhomogeneous object is implemented in each iteration but it leads to a slow segmentation speed with high computational cost. In contrast, work by (Mahmoodi, 2003) uses the nonlinear diffusion

function together with the wavelet thresholding method to reduce image noise. The authors propose a weighted diffusivity function that incorporates contextual discontinuities in the image. The diffusivity function is then applied on local image features to improve feature preservation capability along with noise removal. However, the method concentrates on image de-noising without considering object segmentation in the image. Davatzikos, Tao and Shen (2003) incorporate the nonlinear function into shape-based segmentation to segment different anatomical structures in medical images. They enforce the nonlinear function into global and local shape regularization. However, the method segments the exterior part of the object without considering the inner structure. It also incorporates the shape-based segmentation technique, which requires prior knowledge and an increase in computational cost.

This paper introduces a new ACM with fractional sinc function to reduce the intensity inhomogeneity problem and improve medical image segmentation at a low computational cost. The fractional sinc function is the generalization of nonlinear. The sinc method deals with problems whose solutions may have singularities or boundary layers. The fractional function, on the other hand, models a relationship in which changes in the image texture give the same proportional changes in the movement of the contour evolution. In other words, a contour evolves despite changes in the image region's intensity. These changes commonly occur in images affected by the intensity inhomogeneity problem. The nonlinear applied in the proposed method provides the most flexible contour-fitting functionality in the image. Besides, the sinc method is responsible for solving problems with weak pixels found in the region which lead to missing edges (Sertan & Aydin, 2015). Therefore, the application of the fractional sinc function, which is nonlinear, has the capability of providing an improved bending effect and rapid contour movement during its evolution, a result that is not obtained using normal nonlinear diffusion (Yue et al., 2006). Furthermore, the fractional sinc function embedded with the Gaussian filter is also capable of noise reduction, edge enhancement, and preservation in the image. In the proposed method, this function is embedded within the global and local ACM energies to provide a stable contour evolution and reduce computational cost. This purpose is accomplished because the application of the function within the global energy ensures flexible contour movement, which enables effective bending through an intensity inhomogeneity interface. This leads to reducing the computational cost and thus speeding up the segmentation process. As the proposed method works within the level set framework, the fractional Euler Lagrance is implemented to minimize the energy function. This is to make sure the level set contour/curve stops exactly on the object boundary in achieving improved segmentation. The exponential regression of fractional sinc function is locally adapted to enable the function to slow down the contour movement when it is near the object boundary.

The proposed Fractional Sinc method (FSM) has many advantages. First, FSM is applied in the contour to achieve rapid movement with better bending effects. These effects speed up the segmentation process, thereby reducing the computational cost. Second, the proposed function smoothes the image texture while preserving its edges and enhancing inhomogeneous object classification in the affected regions. Third, improved segmentation in the intensity inhomogeneity interface is accomplished when the fractional sinc function is implemented within the global and local ACMs and the energy is minimized based on the implementation of fractional Euler Lagrance.

THE PROPOSED METHOD

In the traditional ACM, the Gaussian filter is used to smooth the image texture for image segmentation and is normally implemented using the linear function. The filter in the region-based contours is responsible for stopping the contour movement at the correct object boundary. The Gaussian filter tends to overlook neighboring pixels with less prominent

gradients because it moves in straight lines. As a result, identification of the object boundary is less accurate. This method applies the fractional function using the sinc method, which is nonlinear, to produce an efficient interpolation technique. The interpolation technique is a method of constructing new data points within known data points. The technique is performed with contour or curve fitting to achieve improved segmentation of the object to be segmented. Moreover, the collaboration of the interpolation technique of the sinc method with the Gaussian process will allow the contour to pass exactly through the given set or sampling of pixels in a region and enable non-straight rapid contour movement following the image gradient while moving along the identified object boundary. Sinc(t) of order α, (Sinc$_\alpha$), defined as:

$$\sin c_\alpha(t) = \frac{\sin_\alpha(t)}{t}, \qquad t \neq 0$$

$$= \sum_{n=0}^{\infty} \frac{(-1)^n t^{(2-\alpha)n}}{\Gamma((2-\alpha)n+2)},$$

(10)

$$\sin_\alpha(t) = \sum_{n=0}^{\infty} \frac{t^{n-\alpha}}{\Gamma(n-\alpha+1)} \sin((n-\alpha)\frac{\pi}{2})$$

$$= \sum_{n=0}^{\infty} \frac{(-1)^n t^{(2-\alpha)n+1}}{\Gamma((2-\alpha)n+2)},$$

(11)

where Γ is the gamma function, t is the variable and $\alpha \in (0,1)$ is a parameter. The sinc$_\alpha$ function, also called the sampling function, is a function that arises regularly in the theory of Fourier transforms and signal processing, consequently it has many advantages. It has been attached to construct the fractional-delay filters. Fractional-delay filters are types of digital filter equipped for bandlimited fulfillment. Bandlimited fulfillment is a technique for scheming a signal sample at a qualitative point in time, even if it is established somewhere between two sampling points. The extent of the sample ejected is exact because the signal is bandlimited to half the sampling rate. This results in the continuous-time signal being exactly renovated from the sampled data. Moreover, the limit of the sinc function is the Heaviside function as given by:

$$\lim_{t \to 0} \operatorname{sinc}(t) = H(t) = \begin{cases} 1 & t \geq 0 \\ 0 & t < 0 \end{cases}.$$

(12)

The fractional calculus using the sinc method provides a better bending capability and fits the contour movement in the image where the contour movement is more flexible. Bending capability enables the contour to effectively and rapidly move toward the object in the image. The general procedure for nonlinear fractional sinc function is defined by the following recursive equation:

$$S_n = \alpha I_n + (1-\alpha)S_n - 1; \qquad 0 \leq \alpha \leq 1$$

49

where $\{I_n\}$ is the image to be processed, S_n is the processed result for the nth step, and α is the smoothing coefficient. The nonlinear has the capability of protecting and preserving the detail in the images and reducing the image noise. When used after several iterations, Eq. (13) leads to the following equation:

$$S_n = \alpha \sum_{i=1}^{n} \beta^{n-i} I_i + \beta^n S_0, \qquad \beta = 1 - \alpha$$

where the processing result is a weighted sum of all samples with exponential decreasing weights. Eq. (14) has one parameter that meets the algorithm requirements regardless of the number of inputs. The current method proposes the implementation of the control parameter of α with two variables which are embedded in the proposed ACM's global and local energies and are responsible for adjusting the contour movement forward and backward depending on the medical image's characteristics. The variables of the control parameters are adjusted in both the global and local energies to obtain satisfying results. Let C be a contour in an image Ω. The complete energy is defined as follows:

$$F(C, d_1, d_2) = \lambda_1 \int_{in(C)} G(x)|I(y) - d_1(x)|^{\alpha^{x*y}} dxdy$$

$$+\lambda_2 \int_{out(C)} G(x)|I(y) - d_2(x)|^{\alpha^{x*y}} dxdy + \mu. Length(C)$$

where λ_1 and λ_2 are two positive parameters, $G(x)$ is the Gaussian filter function in the proposed method and d_1, d_2 are defined by:

$$d_1(\phi) = \frac{\int_\Omega I(x).\sin c_\alpha(\phi)dx}{\int_\Omega \sin c_\alpha(\phi)dx}, \qquad d_2(\phi) = \frac{\int_\Omega I(x).(1 - \sin c_\alpha(\phi))dx}{\int_\Omega (1 - \sin c_\alpha(\phi))dx}$$

Accordingly, d in Eq.(16) is not a constant value because it leads to linearity in a homogeneous environment. All locations in the image, including the edges, are equally smoothed (Zhang et al., 2009; 2010; 2013) when linearity occurs. This phenomenon cannot happen in medical images because every tiny image detail contains useful information. The level set method is implemented to solve the problem of topological changes in the ACM. Therefore, with the level set method, the new equation is given as follows:

$$F(\phi, d_1, d_2) = \lambda_1 \int_{in(\phi)} G(x)|I(y) - d_1(x)|^{\alpha^{x*y}} sinc_\alpha(\phi)dxdy$$

$$+ \lambda_2 \int_{out(\phi)} G(x) |I(y) - d_2(x)|^{\alpha^{x*y}} \left(1 - sinc_\alpha(\phi)\right) dx dy$$

$$+ \mu . Length(\phi)$$

(17)

where $sinc_\alpha(\phi)$ is based on Heaviside function. As the proposed method works within the level set method (LSM) framework, the level set function (LSF) of LSM normally requires the contour placement to be frequently re-initialized to maintain contour evolution stability. However, this technique requires complex computations to ensure that the evolving LSF is close to the signed distance function cost (Li et. al, 2005; 2010). Hence, the methods currently applying the re-initialization technique are faced with heavy computations. This study proposes an alternative technique by applying the Gaussian filter with fractional sinc function in each contour movement. This technique provides rapid and dynamic movement, which speeds up the segmentation process. Moreover, Gaussian filtering is used to enhance and preserve the edge, thereby maintaining the image structure. The edge is preserved toward the direction of the object boundary. The computational requirement for separating inhomogeneous objects within regions is simplified by applying the fractional sinc function in the Gaussian filter modification. This is given by:

$$I(x) - (d_1 + d_2)^{\alpha^{x*y}}$$

(18)

where d_1 and d_2 are the two regions, and $I(x)$ is the original image. For a better segmentation process, the overall equation is applied to the image to improve the image intensity separation in each region. The power of α is the control parameter of the sinc function with two variable numbers which is based on exponential regression. If a large number is given to the α, the contour will move further toward the segmented object boundary. If a small number is used, the contour will move nearer the segmented object. The choice of input for α depends on the distribution severity of the image intensity. This input needs to be properly tuned. The contour does not stop at the exact object boundaries when only global energy is utilized. To solve this problem, the energy function needs to be minimized where the level set contour must be on the object boundary. To realize this, we implement the distance measure based on the Euler Lagrange technique. As the proposed method is based on the fractional sinc method, the equation for distance measure as stated in the third line of Eq. (17) is given by:

$$Length(\phi) = \mu L_{f\alpha}(\phi)$$

(19)

where $L_{f\alpha}(\phi)$ is the distance measure based on fractional sinc function and is given by;

$$F_\alpha(\phi) = \int_\Omega |\nabla^\alpha \phi(x,y)|^\alpha sinc_\alpha dx dy$$

(20)

To minimize the energy function, $F_\alpha(\phi) = 0$ to make sure the contour is placed exactly on the object boundary.

The algorithm for our proposed method can be summarized in the following steps:

1. The contour is initialized based on the curve evolution

$$\mu = \begin{cases} d_1 & x \in \Omega_{in} \\ d_2 & x \in \Omega_{out} \end{cases}$$

where d is not the constant used to implement the nonlinear diffusion concept.

2. d_1 and d_2 are computed based on Eq. (16).
3. The contour evolves based on the fractional sync function represented by $sinc_\alpha$, $\alpha > 0$.
4. The LSF is regularized based on the local properties.
5. The evolution of the LSF is checked for convergence. If the evolution does not converge, step number 2 is repeated.

In step 3, x and y are the control parameters of α which are adjusted to obtain better contour bending effects and rapid movement toward the boundary of the object. Giving a larger number of x and y parameters (i.e., more than 5) moves the contour far from the boundary. A too small input number (i.e., less than 1) draws the contour near or flat at the boundary of the object of interest. The nonlinear applied on the contour with the fractional sinc function moves it forward and backward until the level set property is equal to $|\nabla\phi| = 1$. The fractional sinc function parameter works well when the local energy is efficiently adapted at the area with a high gradient level.

EXPERIMENTS & RESULTS

The experiment was designed using MATLAB R (2008b) on 2.5 GHz with Intel Processor i5 according to the implementation framework. Regardless of the image modalities, these experiments aimed to evaluate the proposed method's accuracy in segmenting objects in medical images affected by the intensity inhomogeneity problem. The current experiment used medical images as the datasets and they are magnetic resonance imaging (MRI), computerized tomography (CT) scan, microscopic imaging, ultrasound imaging, and x-ray imaging. The CT scan image contained the least noise among these medical images. The object boundary was clearly seen in this image. Therefore, boundary leakage was not a problem. However, the interior parts of the object in the CT scan image often contained more noise and suffered from the intensity inhomogeneity problem. Both the interior and exterior parts of the objects in the other image types suffered from boundary leakages and intensity inhomogeneities. The medical images used in this study are taken from the database of image clef from the year 2010 to year 2012. Two ACM methods were used to assess the proposed algorithm performance: Chan - Vese (Chan & Vese, 2001) and Selective Global Local Active Contour Model (SGLACM) (Zhang et al., 2010) methods. The C–V method is a region-based ACM that incurs high computational cost and produces over segmentation in dealing with intensity inhomogeneity. The SGLACM method manages to address the C–V method's deficiencies but does not provide contour stability during its evolution. To address the stability issue, the DRLSE method introduces the distance measurement term based on local energy. However, the DRLSE method does not segment medical images with a severe intensity inhomogeneity problem. The DRLSE code used in this paper is taken from Chumning Li's homepage, the C-V code is taken from the Mathworks website and the SGLACM code is taken from the Zhang Kaihua homepage.

The experimental conducted in the next section investigated the proposed method's effectiveness in segmenting four medical images that suffer from the inhomogeneity problem. These images were produced from MRI, CT scan, ultrasound, and x-ray. The performance of the proposed method in terms of segmentation accuracy and processing speed was then compared with that of related baseline methods (i.e., SGLACM and C–V).

This section further demonstrated the proposed method's capability to segment a variety of medical images from different modalities with the aim to achieve improved segmentation within intensity inhomogeneity interface. We expect the outcome as a clean image with the initial contour wrap around the object of interest. A clean outcome of segmentation in this study is where only the object in the image is segmented without segmenting other unwanted regions regardless the intensity inhomogeneity problems. The images used in the experiments were MRI images of a brain and a heart, a CT scan image of a brain, ultrasound images of a heart, appendix and breast cyst and x-ray images of blood vessels. The C–V method is among the popular methods currently used in medical image segmentation. The SGLACM method, meanwhile, combines both edge-based and region-based ACMs by using a hybrid concept similar to the proposed method. Hence, the C–V and SGLACM methods were used as the baseline methods in this study. Fig.1 below at the first row illustrated the initial contour for the three methods involved in the experiment. For every experiments executed in this section will be using the same placement of initial contour. The initial contour is produced differently among methods of ACM depending on its nature of implementation. At the first row of Fig.1 illustrated the initial contour placement for C-V, SGLACM and our method respectively. Initial contour placement of our method is similar to initial contour of SGLACM. However, the result obtained from our method is different from SGLACM due to the rapid movement and bending capability provided by the proposed method. The initial contour used throughout the experiment in this study is maintained as shown in Fig. 2, Fig.3 and others.

The first experiment began with the segmentation of an MRI image of a brain which later supported by two CT scan images of brain. Both MRI and CT scan images had less noise compared to the microscopic image of the two cells. However, images present were darker and had many sub-regions except for the second image of CT scan that focusing on the internal part of the white flare which result in a brighter environment. The internal region of brain images are suffered from the intensity inhomogeneity problem that create a challenging situation in segmenting the white flare. The segmentation results are shown in Fig. 1, Fiq.2 and Fig. 3 respectively. In experiments conducted in Fig.1 to Fig.3, the parameter of α that represent the sinc_α function (Eq.17) is adjusted to 0.077 and the parameter of sigma σ is adjusted to 1. If the sigma is chosen as a big number the initial contour may move dynamically and may disappeared without segmenting the object of interest. This is due to the smooth effect on the image texture which is high that may push the contour to move rapidly thus disappear from the image. On the other hand, the parameter α of sinc_α function is given as 0.077 due to the level of noise which is less when compared to the microscopic image of cell. The first column in Fig.1 shows that the C–V method successfully segmented the image. The method highly utilized the global energy. Hence, in internal sub-regions with intensity inhomogeneity, the method tended to also segment unwanted regions and produced over-segmentation. The SGLACM method only segmented the external part of the brain image. The segmentation result of the proposed approach in the third column of Fig. 1 illustrates a smooth segmentation outcome. Both the exterior and interior parts of the brain were successfully segmented. Application of the fractional sinc function in the Gaussian filter also improved the image's appearance. The region was smoother, the edges were clearer, and the image structure was preserved. As a result, the proposed method successfully addressed the intensity

inhomogeneity problem in the internal part of the image and alleviated the oversegmentation problem. Accordingly, the MRI brain was segmented in 50 iterations within 0.66 s. The proposed method segmented the image with a lower computational cost compared to the baseline methods. The C–V method made 300 iterations within 7.28 s. The SGLACM method completed the segmentation in 120 iterations within 1.03 s.
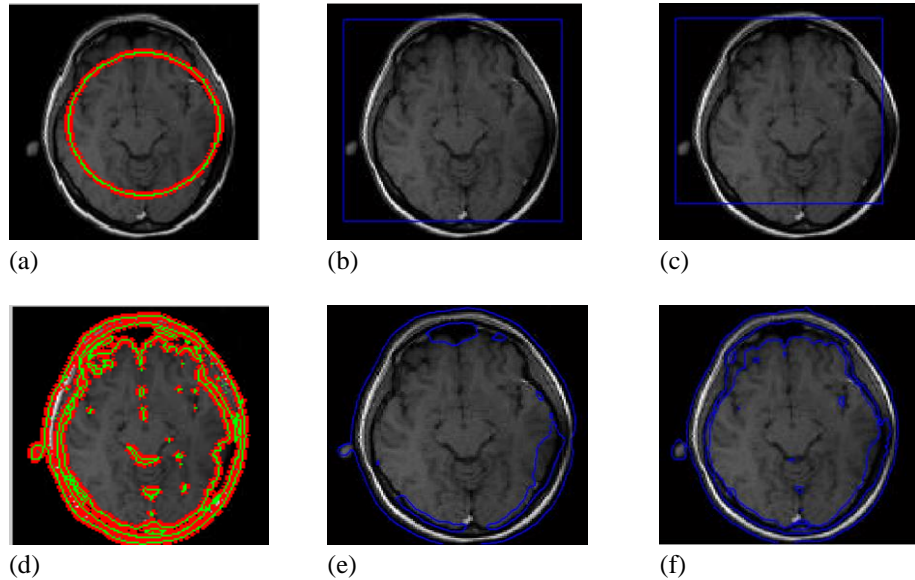

FIGURE 1. Brain MRI image segmentation. The final results using the C–V, SGLACM, and proposed methods are shown in the first, second, and third columns when $\alpha=0.077$ and $\sigma = 1.0$, respectively. The first row shows the initial contour and will be applied throughout the experiments.

Fig.2 illustrates the segmentation outcome for a CT scan image of a brain. The image is used to support the first experiment with the MRI image of a brain, where the image also contained numerous sub-regions which led to over sampling of the initial contour, possibly segmenting the unwanted regions as well. However, unlike the MRI image of the brain, the interior parts of the sub-regions were surrounded with a bright intensity (Fig.2). The C–V method produced the segmentation of unwanted regions and completed the segmentation in 50 iterations within 2.77 s, and this is shown in the first column of Fig.2. The SGLACM method produced a similar outcome, where only the exterior part of the brain was segmented in the MRI image. The method completed the segmentation in 120 iterations within 1.6 s. The proposed method produced a cleaner outcome with segmentation of both the exterior and interior parts in 40 iterations within 1.01 s.
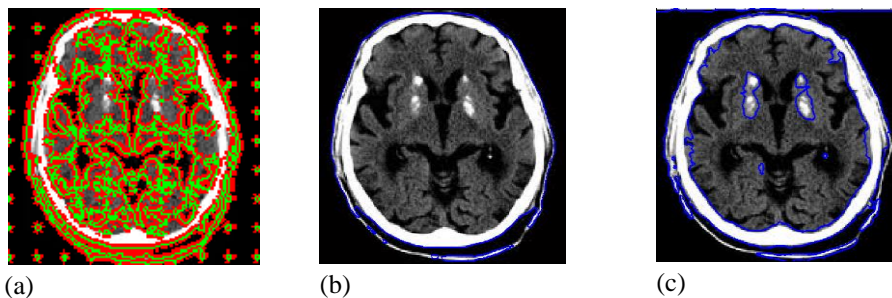

FIGURE 2. CT scan image of brain segmentation. The final results using the C–V, SGLACM, and proposed methods are shown in the first, second, and third columns when $\alpha=0.077$ $\sigma = 1.0$, respectively.

54

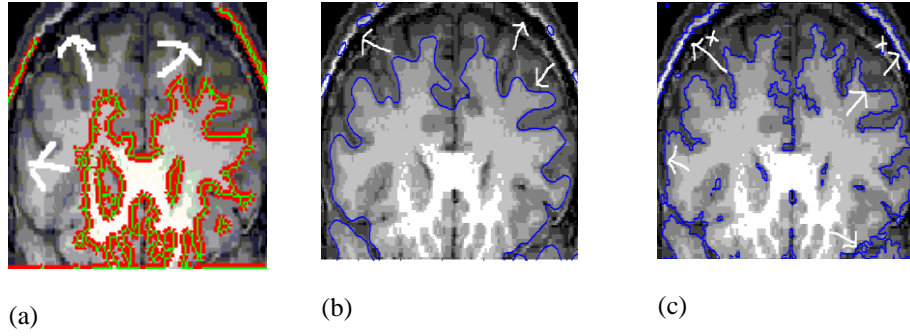(a)   (b)   (c)

FIGURE 3. Segmentation of a second CT scan image of a brain that focus on the white flare. The final results using the C–V, SGLACM, and proposed methods are shown in the first, second, and third columns when α=0.077 and σ = 1.0, respectively.

The experiment was continued with another CT scan image of a brain, but this time the image focused on the white flare in the brain. The aim was to show the accuracy of segmentation provided by the proposed method in segmenting each of the white flares existing in the brain image. The texture of the image was smooth but, the classification of the intensity levels occurring in the image was challenging, where the initial contour may not have correctly moved toward the white flare and segmented each of the white flares in the image. The parameter of sinc_α function and the parameter of sigma used here was the same as used in Fig.2 and Fig.3 as the nature of the image was the same. Among the results obtained, our method presented an outcome which, situated at the last column in Fig.3, showed better accuracy when compared to the outcome using the C-V method in the first column and the SGLACM method in the second column. Our method did not produce any unwanted segmented regions and the thin long white flare labelled "x" in Fig.5 (last column) was excellently segmented compared to other methods where the white flare was not successfully segmented. The C-V method, due its intensity inhomogeneity problem, did not segment the white flare in the image successfully. On the other hand, the SGLACM method produced segmentation which was less accurate with some of the white flare, as shown by the arrow, not being successfully segmented. In terms of speed, our method managed to complete the segmentation process within 40 iterations in 0.8 s whereas the C-V method took 300 iterations in 6.2 s and the SGLACM method took 60 iterations in 0.9 s.

The experiment using the MRI image of a heart was then conducted. We produced two MRI images of the heart with different texture and from a different angle. Both images revealed a slightly different texture than the earlier images. They also suffered from a high noise level with severe intensity inhomogeneity leading to weak edges. The hole in the center revealed a similar gradient level to the background with dark intensity, which made the segmentation process more challenging. Due to the texture of both images being unclear and having more intensity levels which were not homogeneous, we adjusted the sinc_α parameter to be bigger, at 0.084, while the sigma σ was maintained at 1. In this situation the interpolation process of fractional sinc function would better classify the inhomogenous objects in a region. The experimental results for the MRI image of a heart are shown in Fig.4 and Fig.5. The segmentation results using the C–V, SGLACM, and proposed methods are shown in the first, second, and third columns, respectively, in both Fig.4 and Fig.5. The segmentation outcomes were similar in the C–V and the proposed methods for both images in Fig.4 and Fig.5. The proposed method demonstrated a cleaner and more defined segmentation outcome without any oversampling. This result indicated a significant reduction in intensity inhomogeneity in the image. For the image in Fig.4, the C–V method made 100 iterations within 3.68 s to complete the segmentation, whereas the proposed method segmented the heart object in the MRI image with only 40 iterations in 1.7 s. On the other hand the C-V method completed the segmentation

of the image in Fig.5 within 70 iterations in 2.11 s, while our proposed method completed the segmentation within 60 iterations in 1.2 s. The SGLACM method, which made 120 iterations in 0.95 s for the image in Fig.4 and 60 iterations in 1.1 s for the image in Fig.5, only segmented the outer part of the heart object and did not segment the hole in the image's center.
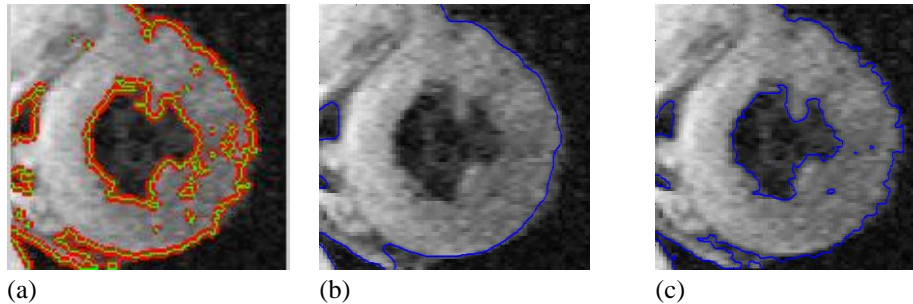

(a)   (b)   (c)

FIGURE 4. Experiment on the MRI image of a heart. The final results using the C–V, SGLACM, and proposed methods are shown in the first, second, and third columns for α=0.084 and σ = 1.0, respectively.
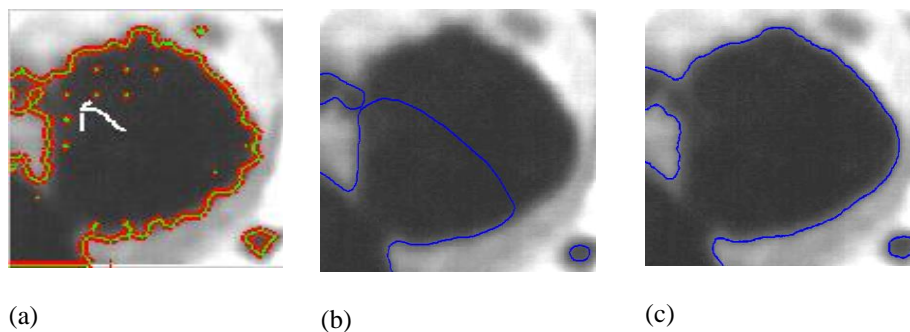

(a)   (b)   (c)

FIGURE 5. Experiment on another MRI image of a heart in different angle. The final results using the C–V, SGLACM, and proposed methods are shown in the first, second, and third columns for α=0.084 and σ = 1.0, respectively.

     The experiment continued with three ultrasound images that represented an image of a liver in Fig.6, image of an appendix in Fig.7 and image of a breast cyst in Fig.8. Ultrasound images are known to be the noisiest among the medical images. To conduct the experiments on these ultrasound images, we adjusted the $sinc_\alpha$ to 0.1, which is much larger, and sigma σ to 5. This was due to the nature of the image, which was rough and had severe intensity inhomogeneity. Moreover, its intensity distribution was not homogeneous, its object boundary was very weak, and it had many missing edges. Besides, the liver image was particularly dark with a complex and rough texture, which posed a challenging situation for any segmentation process. The segmentation outcomes obtained from this experiment are depicted in Fig. 8. As expected, the C-V method displayed many overlapping pixels in the image's regions with 250 iterations in 7.28 s. The SGLACM method only segmented the image exterior with 120 iterations in 0.82 s. Although selective global and local ACM was applied, the contour did not segment the liver object because of the complex image texture. The proposed method demonstrated an impressive outcome in the third column of Fig.6. Without any over sampling, the method accurately segmented the ultrasound image of a liver with 50 iterations in 0.78 s.
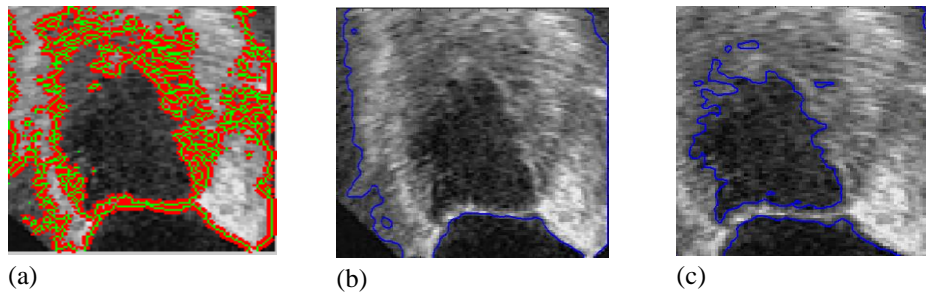
FIGURE 6. Experiment of an ultrasound image of a liver. The final results using the C–V, SGLACM, and proposed methods are shown in the first, second, and third columns, respectively. The parameter of α=0.1 and σ is 5.

The experiment was repeated on an ultrasound image of an appendix to further support the consistency of the experimental findings on ultrasound images. This image of an appendix was more challenging to segment because its texture was more complex and darker than the previous images. The appendix object was labeled "A". Much noise and overlapping pixels surrounded the object, and the quality of this ultrasound image was very low. Hence, the σ values of the proposed method were set larger than usual with $\sigma = 5$ as mentioned earlier. The segmentation results of the appendix object are shown in Fig.7. The C–V method produced a severe over segmentation effect, which made its segmentation result less successful. The SGLACM method only segmented the exterior image border, ignoring the segmentation of the appendix object. A successful appendix object segmentation was demonstrated by the proposed method (third column, Fig.7) with a significantly less over sampling effect than with the C–V method. In terms of the time taken to complete the segmentation, the proposed method took the least time among all the methods. The proposed method took only 40 iterations within 1.21 s, whereas the C–V method completed the segmentation in 140 iterations within 3.23 s. The SGLACM method took about 120 iterations within 1.68 s.
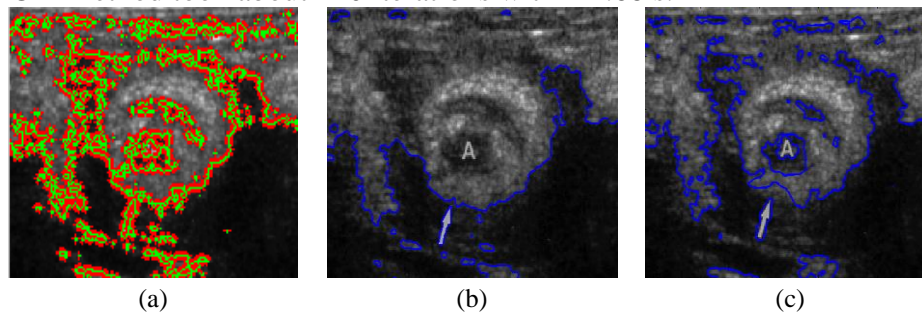

FIGURE 7. Experiments on ultrasound image of appendix. The final results using the C–V, SGLACM, and proposed methods are shown in the first, second, and third columns, respectively. The parameter of α=0.1 and $\sigma = 5$.

Another ultrasound image is shown which represents the image of breast cyst in Fig.10. The reason is to support the experiments conducted earlier and to observe the efficiency of the proposed method. As the nature of the ultrasound image is the same as previous ultrasound images, the parameters used for α and σ are the same as those used in Fig.6 and Fig.7. Based on the outcome obtained, as shown in Fig.8, our method produced a cleaner outcome with reduced intensity inhomogeneity and managed to successfully segment the cyst within 40 iterations in 1.2 s. On the other hand, the C-V method segmented the cyst object within 250 iterations in 8 s but produced segmentation of unwanted regions. SGLACM only segmented

the outer part but did not manage to segment the cyst object, and this was done within 50 iterations in 1.31 s.
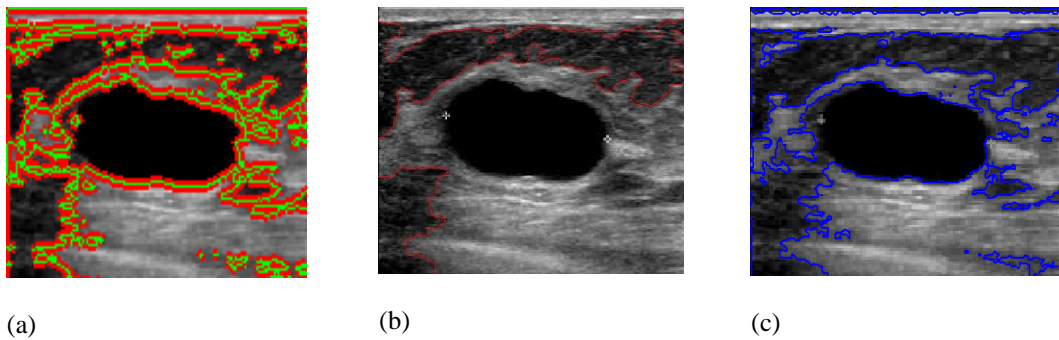

(a)   (b)   (c)

FIGURE 8. Experiments on ultrasound image of breast cysts. The final results using the C–V, SGLACM, and proposed methods are shown in the first, second, and third columns, respectively. The parameter of α=0.1 and σ = 5.

The final experiment was conducted on x-ray images of blood vessels. Unlike the other images, these images were distinctive with a long and winding structure. The background of both images had a slightly brighter intensity than the interior region of the vessels. The texture of the image was smooth and the intensity level that represented the background of the vessel object was slightly similar where the intensity level was difficult to recognize. Thus, we adjusted the α to 0.06 and the σ was adjusted to 3.

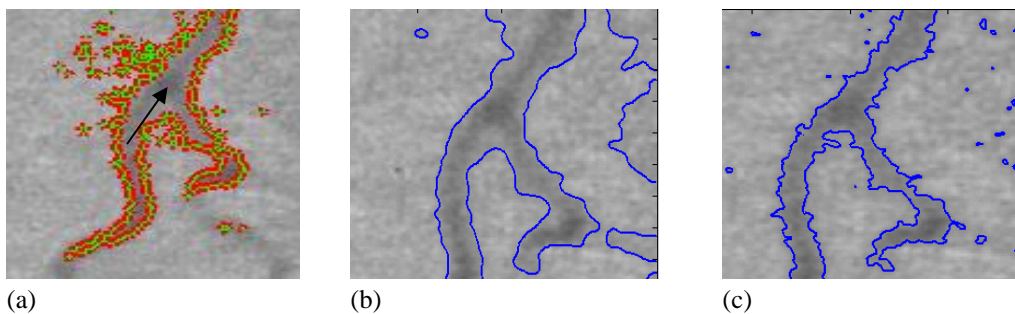(a)   (b)   (c)

FIGURE 9. Experiments on X-ray images of thin and winding blood vessels. The final results using the C-V, SGLACM, and proposed methods are shown in the first, second, and third columns, respectively. The parameter of α=0.06 and σ = 3.

The segmentation results for these images are shown in Figs.9 and 10. The boundary of the long and thin vessels suffered from the intensity inhomogeneity problem, which made the segmentation arduous. The SGLACM method (second column, Fig.9) did not accurately segment the blood vessel. In this case, the contour did not stop on the exact blood vessel boundary. To complete the segmentation process, the method made 120 iterations within 2.02 s. The C-V method did not successfully segment the vessel and failed to identify the area badly affected by the intensity inhomogeneity problem. This area is indicated by an arrow in the first column. To complete the segmentation, the C-V method made 300 iterations within 2.68 s. Using the proposed method, an accurate segmentation outcome for the blood vessel was achieved with a lower computational cost. The method made only 40 iterations within 1.1 s. A similar experiment was repeated on another blood vessel for consistency purposes (Fig.10).

The image in Fig.10 illustrates an intensity inhomogeneity problem together with some subsequent pixels weak in intensity in the vessel. All the methods successfully segmented the

58

blood vessel, albeit with different computational times. The C-V method completed the segmentation process in 50 iterations within 8.4 s. It also encountered some segmentation difficulties along the vessel boundary because of the intensity inhomogeneity effect. In contrast, the SGLACM method made about 40 iterations in 6.8 s to complete the vessel segmentation. The proposed method completed a successful blood vessel segmentation in just 30 iterations within 5.4 s. This computational time was the shortest completion time achieved among the methods.
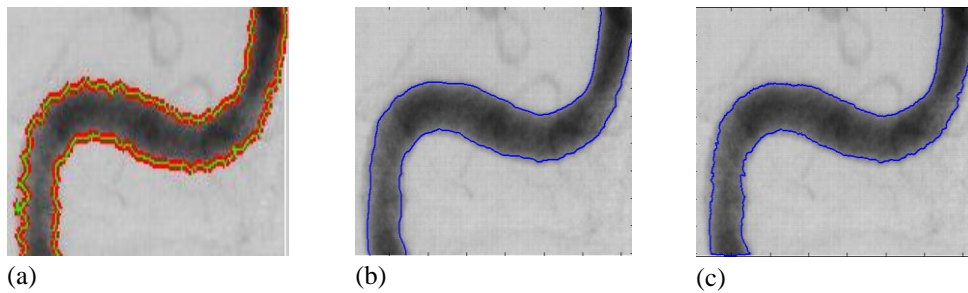

(a)   (b)   (c)

FIGURE 10. Experiments on the second type of blood vessel X-ray images. The final results using the C–V, SGLACM, and proposed methods are shown in the first, second, and third columns, respectively. The parameter of α=0.06 and σ = 3.

Speed, aside from improving the segmentation, was also important in completing the segmentation process. The proposed method produced a satisfactory segmentation outcome in reducing the processing time required to complete successful segmentation.

DISCUSSION

This section discusses the analysis of the results obtained from the experiments on five medical image modalities. Most of the images used in the experiments suffered from intensity inhomogeneity problems. Hence, some critical edges along the object boundary became weak or missing and led to gaps at the boundary. Among the medical images used in this paper, the CT scan image has the least noise, especially at the exterior part of the object. Other images, such as those from MRI, microscopic imaging, ultrasound imaging, and x-ray imaging have much noise, which leads to the intensity inhomogeneity problem. The proposed method aims to reduce the intensity inhomogeneity problem, thereby improving the segmentation of objects of interest in medical images using a shorter processing time.

This study introduces the use of the fractional sinc function of order α with ACM because it removes noise in an image while maintaining the edges of its structure. The use of the sinc method together with the fractional function is further introduced for flexible contour movement with an improved bending effect during its evolution. This bending flexibility enables the contours to easily move forward and backward toward the object of interest and to quickly segment the object. Moreover, the sinc method with fractional function has the strength to rapidly move the contour within the intensity inhomogeneity interface toward the object. It further moves the contour more slowly when it is near the object boundary. Consequently, the contour locally adapts at the boundary interface for improved segmentation results.

The first experiment was conducted on four different modalities which involves various human organ images (i.e., MRI, CT scan, ultrasound, and x-ray). The experiments were conducted to support the use of the nonlinear function in the proposed method. Each image had different characteristics (i.e., dark, blurry, long, thin, and winding). All of the images were affected by noise and the intensity inhomogeneity problem. Some images (i.e. ultrasound

image) had complex and rough textures. The proposed method, which uses the linear with the Gaussian filter, was compared with the C–V and SGLACM methods. The fractional sinc function applied with the proposed method showed an improved segmentation of medical images with an intensity inhomogeneity interface. The proposed method speeds up the segmentation process. The sinc method applied with the fractional function proves that the rapid movement and bending capability of the contour toward the object boundary improves segmentation accuracy with a lower computational cost. Moreover, the fractional sinc function used to modify the Gaussian filter produces enhanced image details, including the edges. This finding is clearly demonstrated in the experiments, where the medical images segmented with the proposed method had less over sampling and improved boundary segmentation accuracy compared with the other approaches. Therefore, the proposed method improves medical image segmentation for various modalities in the intensity inhomogeneity interface with a lower computational cost.

CONCLUSION

A combination of global and local ACMs which uses the fractional sinc function of order α, with exponential regression to speed up contour evolution is presented. This method provides improved bending effects for contour movement during its evolution and enhances an object's boundary edges. This paper proposes the application of the fractional sinc function on the contour during its evolution using both global and local energies. The Gaussian filter is modified with the fractional sinc function to smooth the image and enhance its edges, thereby preserving the image structure. The filter is also used to reduce the oversampling issue produced by region-based ACM on images with intensity inhomogeneity. The contours embedded with the fractional sinc function actively move forward and backward toward the desired object to be closer to the object boundary. A distance measurement based on fractional Euler Lagrance with local energy is implemented to accurately segment the object at its correct boundary within the level set framework. The energy function is minimized as the level set curve meets exactly on the object boundary. Regardless of image modality, the proposed method provides improved segmentation of the object of interest at a lower computational cost than the other common ACM methods.

REFERENCES

Barenblatt G.I, 2001. Self-similar intermediate asymptotics for nonlinear degenerate parabolic free-boundary problems that occur in image processing. *Proceedings of the National Academy of Sciences of the United States of America,* 98(23): 12878-12881.

Barenblatt G.I & Vazquez, J.L, 2004. Nonlinear diffusion and image contour enhancement, *Interfaces Free Boundaries,* 6(2004):31-54.

Caselles. V., Kimmel, R. & Sapiro, G. 1997. Geodesic active contours. *International Journal of Computer Vision,* 22(1):61-79.

Chan, T. & Vese L. 2001. Active Contour Model Without Edges. *IEEE Transactions on Image Processing,* 10(2):266- 277.

Dan, D. & Dali, S. 2012. Sinc-Collocation Method for Solving Linear and Nonlinear System of Second-Order Boundary Value Problems. *Scientific Research Journal,* 2012(3): 1627-1633.

Davatzikos C., Tao, X. & Shen D. 2003. Hierarchical active shape models using the wavelet transform. *IEEE Transaction on Medical Imaging,* 22(3): 414-422.

Hafiane, A., Vieyres, P. & Delbos, A. 2014. Phase-based Probabilistic Active Contour for Nerve Detection in Ultrasound Images for Regional Anesthesia. *Computers in Biology and Medicine Journal*, 52:88-95.

He, S.Z. & Wang, L. 2010. Integrating local distribution information with level set for boundary extraction. *J. Vis. Communication. Image R,* 21:343–354.

Kass, A. & Terzopoulos, D. 1998. Snakes: active contour models. *International Journal of Computer Vision,* 1:321-331.

Li, C.K. Gore, J.C. & Ding, Z. 2008. Minimization of region-scalable fitting energy for image segmentation. *IEEE Trans. Image Process,* vol. 17(10):1940-1949.

Li, C.X., Gui, C. & Fox, M.D. 2005. Level set evolution without re-initialization: A new variational formulation. *Proceedings of the IEEE Conf. Comput. Vis Pattern Recognition,* 1(10):430-436.

Li, C.X., Gui, C. & Fox, M.D. 2010. Distance Regularized level set evolution and its application to image segmentation, *IEEE Trans on Image Processing*, 19(12):3243- 3254.

Mahmoodi, S. 2003. Unsupervised texture segmentation using nonlinear energy optimization method, *Journal of Electronic Imaging*, 15(3):033006.

Patil, P. & Deore, M. 2013. Medical image segmentation: A review. *International Journal of Computer Science and Mobile Computing,* 2: 22-27.

Perona P. & Malik, J. 1990. Scale-space and edge detection using anisotropic diffusion. *IEEE Transactions on Pattern Analysis and Machine Intelligence*, 12(7):629-639.

Sertan A. & Aydin S. 2015. Application of Sinc-Galerkin Method for Solving Space-Fractional Boundary Value Problems, *Journal of Mathematical Problems in Engineering,* 2015.

Wang H. & Mishra C. 2008. Active contours driven by local Gaussian distribution fitting energy, *Signal Processing Journal,* 89(2009):2435-2447.

Xu C, A.Y., & Prince, J.L. 2000. On the relationship between parametric and geometric active contours. *Proceedings of the 34th Asilomar Conf. Signals. Systs., Comput.* Pacific Grove, California:[s.n.].

Yue, Y., Croitoru, M., Bidani, A., Joseph, B. Z, John, W. & Clark, H. W. 2006. Nonlinear Multiscale Wavelet Diffusion for Speckle Suppression and Edge Enhancement in Ultrasound Images. *IEEE Transactions on Medical Imaging,* 25(3): 97.

Zhang, K.H., Song, H. & Zhang, L, 2009. Active contours driven by local image fitting energy. *Pattern Recognition,* 43:1199-1206.

Zhang, K.H., Song, H., Zhang, L. & Zhou,W. 2010. Active contours with selective local or global segmentation: A new formulation and level set method. *Image and Vision Computing,* 28:668-676.

Zhang, K.H., Zhang L., Lam K.M. & Zhang D. 2013. A Local Active Contour Model for Image Segmentation with Intensity Inhomogeneity, *Computer Vision & Pattern Recognition,* 1305.7053.

Norshaliza Kamaruddin
First City University College
No.1, Persiaran Bukit Utama, Bandar Utama
47800 Petaling Jaya, Malaysia.
shaiza.kama@gmail.com